

QCD Corrections to Jet Production in Polarized ep Scattering

E. Mirkes and S. Willfahrt

*Institut für Theoretische Teilchenphysik, Universität Karlsruhe,
D-76128 Karlsruhe, Germany*

Abstract

Next-to-leading order QCD predictions for 1-jet and 2-jet cross sections in polarized deep inelastic scattering at HERA energies are presented. Whereas the QCD corrections to the total polarized cross section are very large, only moderate corrections are found for the dijet cross sections.

1 Introduction

After the confirmation of the surprising EMC result that quarks carry only a little fraction of the nucleon spin the spin structure of a longitudinally proton is actively being studied theoretically and experimentally by several fixed target experiments at CERN, DESY, and SLAC [1]. So far only the inclusive polarized structure functions g_1 and g_2 have been measured. These measurements, however, do not allow to distinguish between the role of quarks and gluon distributions. The measurement of the polarized gluon distribution $\Delta g(x_g, \mu_F^2)$ has become the key experiment in order to understand the QCD properties of the spin of the nucleon. We study here the possible direct measurement of $\Delta g(x_g, \mu_F)$ from dijet events at a HERA collider, in the scenario where both the electron and the proton beam are polarized. The measurement of the 2-jet final state allows for a unique determination of the polarized gluon distribution $\Delta g(\xi, \mu_F)$, in a region, where $x_g \Delta g(x_g)$ is expected to show a maximum [2, 3, 4]. As in the unpolarized case, the gluon distribution enters the 2-jets production cross section at LO thus suggesting such a direct measurement. We will present first results of the full NLO QCD corrections to the 2-jet cross section in this contribution. The numerical results are based on the fully differential $ep \rightarrow n$ jets event generator MEPJET 2.2 [5, 6] which allows to analyze any 1- or 2-jet like observable in polarized ep -scattering in NLO in terms of parton 4-momenta.

The NLO hadronic n -jet cross section is given by

$$d\Delta\sigma_{\text{had}}[\text{n-jet}] = \sum_a \int dx_a \Delta f_a(x_a, \mu_F) \alpha_s^n(\mu_R) \Delta\hat{\sigma}_a(p_0 = x_a P, \mu_R, \mu_F) \quad (1)$$

Here, the polarized hadronic cross section is defined as

$$d\Delta\sigma_{\text{had}}[\text{n-jet}] \equiv \frac{1}{2} (d\sigma_{\text{had}}^{\uparrow\downarrow}[\text{n-jet}] - d\sigma_{\text{had}}^{\uparrow\uparrow}[\text{n-jet}]) \quad (2)$$

where the left arrow in the superscript denotes the polarization of the incoming lepton with respect to the direction of its momentum. The right arrow stands for the polarization of the proton parallel or anti-parallel to the polarization of the incoming lepton. The polarized parton distributions are defined by $\Delta f_a(x_a, \mu_F^2) \equiv f_{a\uparrow}(x_a, \mu_F) - f_{a\downarrow}(x_a, \mu_F)$. Here, $f_{a\uparrow}(f_{a\downarrow})$ denotes the probability to find a parton a in the longitudinally polarized proton whose spin is aligned (anti-aligned) to the proton's spin.

$\Delta\hat{\sigma}_a$ denotes the polarized NLO differential partonic cross section for the subprocess

$$e^\pm(l) + \text{parton } a(p_0) \rightarrow e^\pm(l') + \text{parton } 1(p_1) \dots + \text{parton } n(p_n) \quad (3)$$

with α_s set to one from which collinear initial state singularities have been factorized out at a scale μ_F and have been implicitly included in the scale dependent parton densities $f_a(x_a, \mu_F)$. The following tree level and one loop subprocesses contribute to polarized n -jet production (up to NLO for $n = 1, 2$)

1-jet:	LO	$\mathcal{O}(\alpha_s^0)$:	$e + q \rightarrow e + q$	
1-jet:	NLO	$\mathcal{O}(\alpha_s)$:	$e + q \rightarrow e + q$	1-loop corrections
			+ unresolved contributions from the $\mathcal{O}(\alpha_s)$ 2-parton final states	
2-jets:	LO	$\mathcal{O}(\alpha_s)$:	$e + q \rightarrow e + q + g$	
			$e + g \rightarrow e + q + \bar{q}$	
2-jets:	NLO	$\mathcal{O}(\alpha_s^2)$:	$e + q \rightarrow e + q + g$	1-loop corrections
			$e + g \rightarrow e + q + \bar{q}$	1-loop corrections
			+ unresolved contributions from the $\mathcal{O}(\alpha_s^2)$ 3-parton final states	
3-jets:	LO	$\mathcal{O}(\alpha_s^2)$:	$e + q \rightarrow e + q + g + g$	
			$e + q \rightarrow e + q + q + \bar{q}$	
			$e + g \rightarrow e + q + \bar{q} + g$	

(4)

and the crossing related anti-quark processes with $q \leftrightarrow \bar{q}$.

First discussions about jet production in polarized lepton-hadron scattering can be found in Ref. [7], where jets were defined in the JADE scheme for center of mass energies of 20 GeV, (which is about the energy of the fixed-target EMC experiment at CERN with a polarized muon beam of energy around 220 GeV). Although this energy is too small to observe clear jet structures, the studies in Ref. [7] demonstrated already the unique possibility for a measurement of the polarized gluon density from dijet events in polarized DIS. Prospects for measuring the polarized gluon distribution at HERA energies have been discussed first in [2, 3]. The results have been confirmed with the PEPSI program [8]. An extension of these studies including a first discussion of the QCD corrections to the polarized inclusive and 1-jet cross sections and $\mathcal{O}(\alpha_s^2)$ polarized 3-jet cross sections was presented in Ref [6]. In this contribution, we present first NLO results for dijet cross sections.

1.1 Polarized Jet Cross Sections

Following the theoretical framework for the calculation of NLO jet cross section in unpolarized ep -scattering as explained in depth in Ref. [6], the polarized hadronic 1-jet *exclusive* cross section in the 1-photon exchange up to $\mathcal{O}(\alpha_s)$ reads

$$\begin{aligned}
\Delta\sigma_{\text{had}}[1\text{-jet}] &= \\
&\int_0^1 d\eta \int d\text{PS}^{(l'+1)} \sigma_0 \left[\right. \\
&\left. \left[\sum_{i=q,\bar{q}} e_i^2 \Delta f_i(\eta, \mu_F) \right] \Delta |M_{q \rightarrow q}^{(\text{pc})}|^2 \left(1 + \alpha_s(\mu_R) \mathcal{K}_{q \rightarrow q}(s_{\min}, Q^2) \right) \right. \\
&+ \left. \left[\sum_{i=q,\bar{q}} e_i^2 \Delta C_i^{\overline{\text{MS}}}(\eta, \mu_F, s_{\min}) \right] \alpha_s(\mu_R) \Delta |M_{q \rightarrow q}^{(\text{pc})}|^2 \right] J_{1 \leftarrow 1}(\{p_i\}) \\
&+ \int_0^1 d\eta \int d\text{PS}^{(l'+2)} \sigma_0 (4\pi\alpha_s(\mu_R)) \left[\right. \\
&\left. \left[\sum_{i=q,\bar{q}} e_i^2 \Delta f_i(\eta, \mu_F) \right] \Delta |M_{q \rightarrow qg}^{(\text{pc})}|^2 \right. \\
&+ \left. \left. \left(\sum_{i=q} e_i^2 \right) \Delta f_g(\eta, \mu_F) \Delta |M_{g \rightarrow q\bar{q}}^{(\text{pc})}|^2 \right] \prod_{i < j; 0}^2 \Theta(|s_{ij}| - s_{\min}) J_{1 \leftarrow 2}(\{p_i\}) \right]
\end{aligned} \tag{5}$$

where the Lorentz-invariant phase space measure $d\text{PS}^{(l'+n)}$ is defined in Eq. (9) of Ref. [6] and $\sigma_0 = \pi^2 \alpha^2 / ((p_0 \cdot l) Q^4)$. $J_{1 \leftarrow 1}(\{p_i\})$ and $J_{1 \leftarrow 2}(\{p_i\})$ represents the jet algorithms. The jet algorithm $J_{n \leftarrow n}$ yields one if the original final state n -parton configuration yields n jets satisfying the experimental cuts. $J_{n \leftarrow n}$ can be expressed as a product of a clustering part and an acceptance part [6]. Similarly, the jet algorithm $J_{n \leftarrow n+1}$ evaluates to one if the $(n+1)$ -parton configuration yields n detected jets and vanishes otherwise. More precisely, $J_{n \leftarrow n+1}$ evaluates to one either if one pair of partons is clustered into one jet and the remaining $(n-1)$ partons are well separated from this jet and pass all acceptance criteria (together with the jet) or all $(n+1)$ partons are resolved but one parton does not pass the acceptance cut. For more details see Eqs. (10) and (18), respectively in Ref. [6]. The 1-jet *inclusive* cross section is defined via Eq. (5) by replacing $J_{1 \leftarrow 2}(\{p_i\})$ in the last line by $(J_{1 \leftarrow 2}(\{p_i\}) + J_{2 \leftarrow 2}(\{p_i\}))$, *i.e.* the 1-jet inclusive cross section is defined as the sum of the NLO 1-jet exclusive cross section (as defined in Eq. (5)) plus the LO two jet cross section. The theoretical cutoff parameter s_{\min} is a completely unphysical parameter and the numerical results for any infrared safe observable are insensitive to a reasonable variation for sufficiently small s_{\min} values [5, 6]. The dynamical $\mathcal{K}_{q \rightarrow q}$ factor in Eq. (5) is the same as is unpolarized case given in Eq. (164) in Ref [6]. The polarized squared matrix elements in Eq. (5) are [6]:

$$\Delta |M_{q \rightarrow q}^{(\text{pc})}|^2 = |M_{q \rightarrow q}^{(\text{pv})}|^2 = 32 \left[(p_0 \cdot l)^2 - (p_0 \cdot l')^2 \right] = 8\hat{s}^2 (1 - (1 - y)^2) \tag{6}$$

$$\Delta |M_{q \rightarrow qg}^{(\text{pc})}|^2 = |M_{q \rightarrow qg}^{(\text{pv})}|^2 = \frac{128}{3} (l \cdot l') \frac{(l \cdot p_0)^2 - (l' \cdot p_0)^2 - (l \cdot p_1)^2 + (l' \cdot p_1)^2}{(p_1 \cdot p_2)(p_0 \cdot p_2)} \tag{7}$$

$$\Delta |M_{g \rightarrow q\bar{q}}^{(\text{pc})}|^2 = 16 (l \cdot l') \frac{(l' \cdot p_2)^2 - (l \cdot p_2)^2 + (l' \cdot p_1)^2 - (l \cdot p_1)^2}{(p_0 \cdot p_1)(p_0 \cdot p_2)} \tag{8}$$

Color factors (including the initial state color average) are included in these results.

The structure of the polarized crossing functions $\Delta C_{q,\bar{q}}^{\overline{\text{MS}}}(\eta, \mu_F, s_{\min})$ in Eq. (5) is identical to the structure of the unpolarized crossing functions [9, 6]:

$$\Delta C_a^{\overline{\text{MS}}}(x, \mu_F, s_{\min}) = \left(\frac{N}{2\pi} \right) \left[\Delta A_a(x, \mu_F) \ln(s_{\min}/\mu_F) + \Delta B_a^{\overline{\text{MS}}}(x, \mu_F) \right] \tag{9}$$

with

$$\Delta A_a(x, \mu_F) = \sum_p \Delta A_{p \rightarrow a}(x, \mu_F) \quad \Delta B_a^{\overline{\text{MS}}}(x, \mu_F) = \sum_p \Delta B_{p \rightarrow a}^{\overline{\text{MS}}}(x, \mu_F) \quad (10)$$

The sum runs over $p = q, \bar{q}, g$. More specifically, the polarized crossing functions for valence quarks and sea quarks, which are needed in Eq. (5), can be obtained from Eqs. (27,28) in Ref. [6] by replacing A, B, C by $\Delta A, \Delta B, \Delta C$ respectively. The finite functions $\Delta A_{q \rightarrow q}(x, \mu_F)$ and $\Delta B_{q \rightarrow q}^{\overline{\text{MS}}}(x, \mu_F)$ can be obtained from the r.h.s. of Eqs. (31,35) in Ref. [6] with f_q replaced by Δf_q . The polarized $g \rightarrow q$ induced functions $\Delta A_{g \rightarrow q}(x, \mu_F)$ and $\Delta B_{g \rightarrow q}^{\overline{\text{MS}}}(x, \mu_F)$ are given by

$$\Delta A_{g \rightarrow q} = \int_x^1 \frac{dz}{z} \Delta f_g(x/z, \mu_F) \frac{1}{4} \Delta \hat{P}_{g \rightarrow q}^{(4)}(z) \quad (11)$$

$$\Delta B_{g \rightarrow q}^{\overline{\text{MS}}} = \int_x^1 \frac{dz}{z} \Delta f_g(x/z, \mu_F) \frac{1}{4} \left\{ \Delta \hat{P}_{g \rightarrow q}^{(4)}(z) \ln(1-z) - \Delta \hat{P}_{g \rightarrow q}^{(\epsilon)}(z) \right\} \quad (12)$$

with the polarized Altarelli-Parisi kernels

$$\Delta \hat{P}_{g \rightarrow q}^{(4)}(z) = \frac{1}{3} \Delta P_{q\bar{q} \rightarrow g}^{(4)}(z) = \frac{2}{3} [2z-1] \quad (13)$$

$$\Delta \hat{P}_{g \rightarrow q}^{(\epsilon)}(z) = \frac{1}{3} \Delta P_{g \rightarrow q}^{(\epsilon)}(z) = 0 \quad (14)$$

The corresponding formula to Eq. (5) for the NLO 2-jet cross section is too long to be presented here.

1.2 Numerical Results

In this part we present numerical results for polarized NLO 1- and 2-jet cross sections at HERA energies. Eq. (5) includes all relevant information for the calculation of the fully differential 1-jet or total $\mathcal{O}(\alpha_s)$ polarized cross section.

For the following numerical studies we use a cone algorithm defined in the lab frame with $\Delta R = 1$ and $p_T^{\text{lab}} > 5$ GeV. Events are selected in the Q^2 range of $40 < Q^2 < 2500$ GeV 2 . In addition, we require $0.3 < y < 1$, an energy cut of $E(e') > 5$ GeV on the scattered electron, and a cut on the pseudo-rapidity $\eta = -\ln \tan(\theta/2)$ of the scattered lepton and jets of $|\eta| < 3.5$. The renormalization scale and the factorization scale are set to Q . The results are based on parton distributions from Gehrmann and Stirling (GS) [10] “gluon set A” together with the 2-loop formula for the strong coupling constant.

With these parameters, one obtains 23 pb for the LO 1-jet cross section ($\equiv \sigma_{\text{tot}}^{\text{LO}}$) and -10.4 pb for the NLO 1-jet inclusive cross section¹ ($\equiv \sigma_{\text{tot}}^{\text{NLO}}$).

The origin of these extremely large corrections is investigated in Fig. 1. The Bjorken- x dependence of the corresponding cross sections in Fig. 1a shows that the corrections are dominated by events at small x . As already mentioned the $\mathcal{O}(\alpha_s)$ corrected 1-jet inclusive cross section (solid curve in Fig. 1a) is defined as the sum of the NLO 1-jet exclusive and the LO 2-jet cross section. Fig. 1b shows the x dependence of the hard LO 2-jet contribution. The negative corrections are entirely due to the hard boson-gluon fusion subprocess (lower curve in Fig. 1b), which is negative for $x \lesssim 0.025$, whereas the contribution from the quark-initiated process is positive (but fairly small) over the whole kinematical range. The important observation is that the $\mathcal{O}(\alpha_s)$

¹The difference between the 1-jet (inclusive) cross section and the total ($\mathcal{O}(\alpha_s)$) cross section due to effects discussed in section 4.2 in Ref. [6] are small and will be neglected in the following.

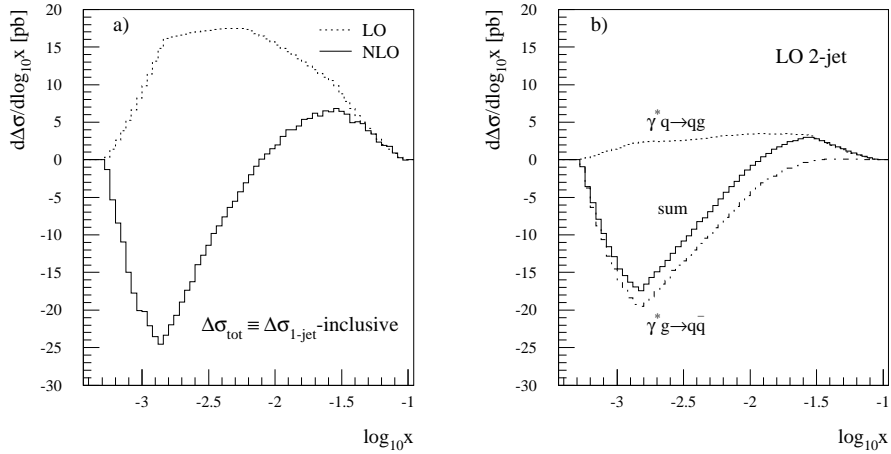


Figure 1: a) Dependence of the polarized LO and NLO 1-jet inclusive cross section as a function of Bjorken x with cuts as described in the text. LO (NLO) results are based on LO (NLO) “gluon set A” parton distributions [10]; b) LO 2-jet contribution to the NLO 1-jet inclusive result in a). Jets are required to have $p_T^{\text{lab}}(j) > 5$ GeV. Results are shown for the quark and gluon initiated subprocesses alone and for the sum.

corrections in Fig. 1a are dominated by these hard 2-jet events, and in particular by the large negative contribution from the boson-gluon fusion subprocess.

In order to compare the feasibility and the sensitivity of the measurement of the spin asymmetry at HERA energies, Fig. 2a compares the asymmetries

$$\langle A_{\text{tot}} \rangle = \frac{\Delta\sigma_{\text{NLO}}^{\text{had}}[\text{tot}]}{\sigma_{\text{NLO}}^{\text{had}}[\text{tot}]} \quad \langle A_{\text{2-jet}} \rangle = \frac{\Delta\sigma^{\text{had}}[2\text{-jet}]}{\sigma^{\text{had}}[2\text{-jet}]} \quad (15)$$

as a function of x . The unpolarized cross sections in the denominators of Eq. (15) are based on NLO GRV [12] parton distribution functions.

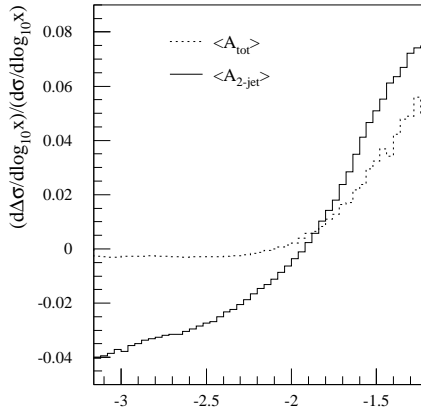


Figure 2: Asymmetries $\langle A_{\text{2-jet}} \rangle$ and $\langle A_{\text{tot}} \rangle$ in Eq. (15) as a function of x .

One observes that the dijet asymmetry $\langle A_{\text{2-jet}} \rangle$ is much larger (up to 3-4%) than the inclusive asymmetry $\langle A_{\text{tot}} \rangle$ in the low x region, which is hardly (or even not at all) constrained by currently available DIS data. Thus, the dijet events from polarized electron and polarized proton collisions

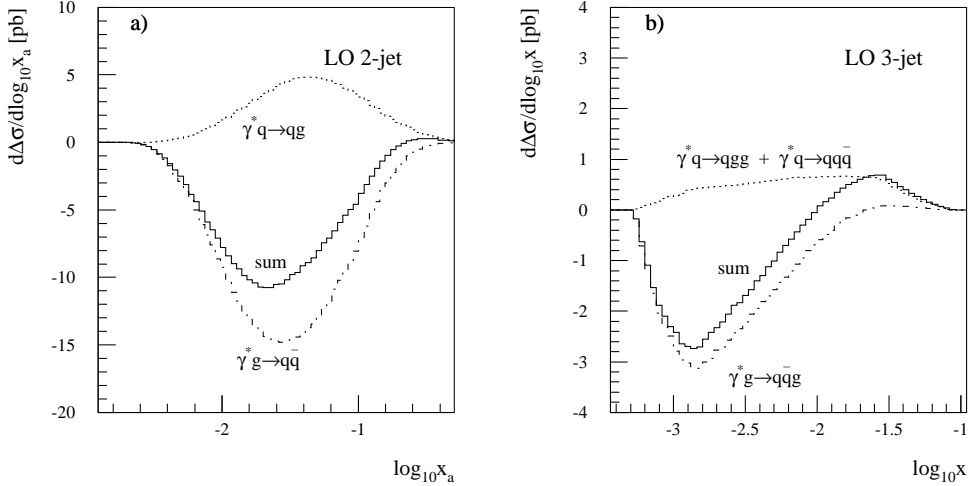


Figure 3: a) Same as Fig. 1b for the x_a ($a = q, g$) distribution, x_a representing the momentum fraction of the incident parton at LO; b) $\mathcal{O}(\alpha_s^2)$ 3-jet contribution with $p_T^{\text{lab}}(j) > 5$ GeV. Results are shown for the quark and gluon initiated subprocesses alone and for the sum.

at HERA are expected to provide the best measurement of the gluon polarization distribution in the small x regime.

For the isolation of polarized parton structure functions we are interested, however, in the fractional momentum x_a of incoming parton a ($a = q, g$), which is related to x by

$$x_a = x \left(1 + s_{jj}/Q^2\right) \quad (16)$$

(s_{jj} denotes the invariant mass squared of the two jets). The corresponding x_a distributions of the polarized 2-jet cross sections are shown in Fig. 3a.

LO predictions for the polarized $\mathcal{O}(\alpha_s^2)$ 3-jet cross sections are shown as a function of Bjorken- x in Fig. 3b. One observes a very similar shape for the gluon and quark initiated subprocesses as already found for the 2-jet results in Fig. 1b. Moreover, the 3-jet cross sections are now suppressed by about a factor five compared to the LO 2-jet cross sections in Fig. 1b. Note that the new gluon initiated subprocess $eg \rightarrow eq\bar{q}$ was responsible for the very large $\mathcal{O}(\alpha_s)$ corrections in the 1-jet inclusive case. There is no such *new* contributing subprocess starting at $\mathcal{O}(\alpha_s^2)$ (see Fig. 3b), which could introduce similarly large corrections to the 2-jet results.

The QCD corrections to the dijet cross sections are investigated in Figs. 4,5. Compared to the previous results for dijet cross sections, jets are required to have transverse momenta of at least 5 GeV in the laboratory frame and in the Breit frame. Furthermore the renormalization scale and the factorization scale are set to $\mu_R = \mu_F = 1/2 \sum_j k_T^B(j)$ [6]. Here $(k_T^B(j))^2$ is defined by $2E_j^2(1 - \cos \theta_{jP})$, where the subscripts j and P denote the jet and proton, respectively (all quantities are defined in the Breit frame). LO (NLO) results are based on LO (NLO) parton distributions from Ref. [10] with the 2-loop formula for the strong coupling constant. With these parameters one obtains a LO (NLO) polarized two jet cross section $\Delta\sigma^{\text{had}}(2\text{-jet})$ of -10.4 pb (-10.0 pb). Thus the higher order corrections are small.

Fig. 4a shows the dependence of the polarized exclusive 2-jet cross section in the cone scheme on Bjorken x in LO and NLO. The effective K -factor close to unity for the exclusive dijet cross section is a consequence of compensating effects in the low x ($K < 1$) and high x ($K > 1$) regime. The dependence on the fractional momentum x_a of incoming parton a ($a = q, g$), which is related

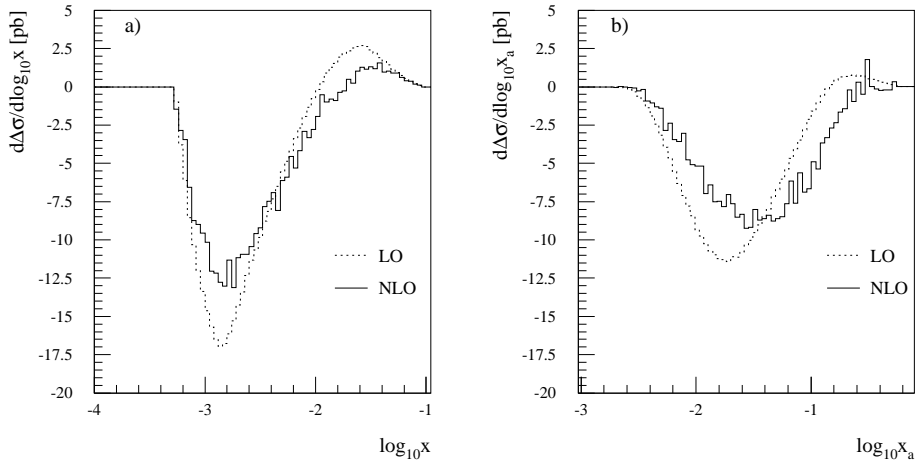


Figure 4: (a) Dependence of the polarized exclusive 2-jet cross section on Bjorken x . Both LO (dashed) and NLO (solid) results are shown. LO (NLO) results are based on LO (NLO) “gluon set A” parton distributions [10]. (b) Same as a) for the x_i distribution, x_i representing the momentum fraction of the incident parton at LO.

by Eq. (16) to Bjorken- x , is shown in Fig. 4b. The NLO distribution is shifted towards larger x_a values compared to the LO result. The s_{jj} distribution in Fig. 5a exhibits fairly large QCD corrections as well. In particular, the invariant mass squared of the two jets is larger at NLO than at LO.

Another observable which exhibits rather large NLO corrections is the the jet rapidity of the most forward jet in the lab frame shown in Fig. 5b. At NLO jets are produced somewhat more forward (in the proton direction) than at LO. Hence, the rapidity cut at $|\eta_j| = 3.5$ has a stronger effect in NLO, which partially explains the K -factor close to one.

We found, that the QCD corrections to the transverse momentum distributions of the jets in both the lab and Breit frame are fairly small. Furthermore, it is shown in Refs. [2, 3, 4] that the 2-jet spin asymmetry is not washed out by hadronization effects. Asymmetry distributions for additional kinematical variables are considered in Ref. [11].

In conclusion, the QCD corrections to dijet cross sections in polarized electron and polarized proton collisions at HERA are found to be moderate. Thus, dijet events can provide a good measurement of the gluon polarization distribution.

References

- [1] A. Magnon, Proceedings of the “*International Workshop on Deep Inelastic Scattering and Related Phenomena*” (DIS96), Rome, April 1996, (QCD162:D41:1996), and references therein.
- [2] F. Kunne, J. Feltesse and E. Mirkes, *Phys. Lett.* **B388** (1996) 832; [hep-ph/9607336].
- [3] A. De Roeck et. al, Proceedings of the “*Workshop on Future Physics at HERA*” Vol. 2 (1996) p. 803, [hep-ph/9610315].

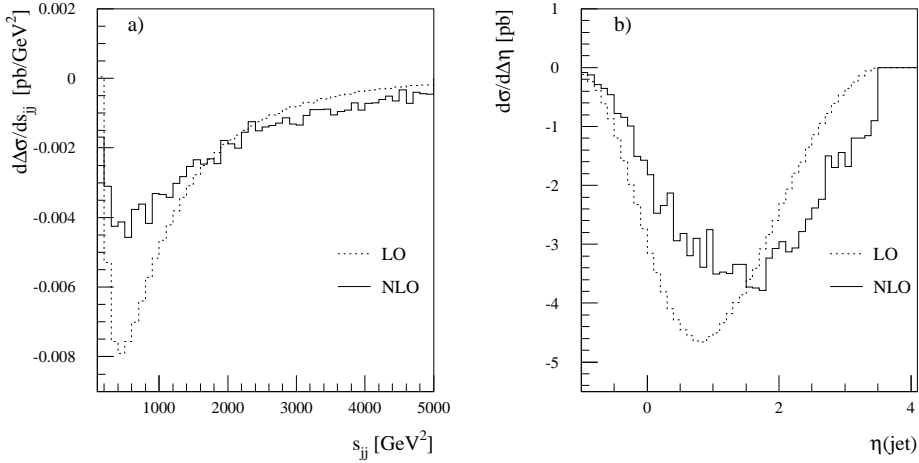


Figure 5: (a) Dijet invariant mass distribution in LO (dashed) and in NLO (solid). (b) Rapidity distribution of the most forward jet in the lab frame. Results are shown in LO (dashed curves) and NLO (solid) for the 2-jet exclusive cross section.

- [4] G. Rädel, A. De Roeck and M. Maul, these proceedings, [hep-ph/9711373].
- [5] E. Mirkes and D. Zeppenfeld, *Phys. Lett.* **B380** (1996) 105, [hep-ph/9511448]; *Acta Phys. Pol.* **B27** (1996) 1393, [hep-ph/9604281].
- [6] E. Mirkes, Habilitationsschrift, [hep-ph/9711224].
- [7] E. Mirkes and C. Ziegler, *Nucl. Phys.* **B429** (1994) 93, [hep-ph/9403410].
- [8] L. Mankiewicz, A. Schäfer, M. Veltri, *Computer Phys. Comm.* **71** (1992) 305.
- [9] W.T. Giele, E.W.N. Glover and D.A. Kosower, *Nucl. Phys.* **B403** (1993) 633.
- [10] T. Gehrmann and J. Stirling, *Phys. Rev.* **D53** (1996) 6100, [hep-ph/9512406].
- [11] M. Maul, A. Schäfer, E. Mirkes and G. Rädel, [hep-ph/9710309].
- [12] M. Glück, E. Reya and A. Vogt, *Zeit. Phys.* **C67** (1995) 433.

